



저작자표시-동일조건변경허락 2.0 대한민국

이용자는 아래의 조건을 따르는 경우에 한하여 자유롭게

- 이 저작물을 복제, 배포, 전송, 전시, 공연 및 방송할 수 있습니다.
- 이차적 저작물을 작성할 수 있습니다.
- 이 저작물을 영리 목적으로 이용할 수 있습니다.

다음과 같은 조건을 따라야 합니다:



저작자표시. 귀하는 원저작자를 표시하여야 합니다.



동일조건변경허락. 귀하가 이 저작물을 개작, 변형 또는 가공했을 경우에는, 이 저작물과 동일한 이용허락조건하에서만 배포할 수 있습니다.

- 귀하는, 이 저작물의 재이용이나 배포의 경우, 이 저작물에 적용된 이용허락조건을 명확하게 나타내어야 합니다.
- 저작권자로부터 별도의 허가를 받으면 이러한 조건들은 적용되지 않습니다.

저작권법에 따른 이용자의 권리는 위의 내용에 의하여 영향을 받지 않습니다.

이것은 [이용허락규약\(Legal Code\)](#)을 이해하기 쉽게 요약한 것입니다.

[Disclaimer](#)

교육학석사 학위논문

**Autofluorescence generation and elimination:  
a lesson from glutaraldehyde**

세포의 자가 형광 발현의 발현과 제거:  
글루타알데히드를 이용한 모델 연구

2013 년 6 월

서울대학교 대학원

과학교육과 화학전공

이 과 훈

**Autofluorescence generation and elimination:  
a lesson from glutaraldehyde**

지도교수 Yu, Junhua

이 논문을 교육학석사 학위논문으로 제출함

2013 년 6 월

서울대학교 대학원  
과학교육과 화학전공  
이 과 훈

이과훈의 교육학석사 학위논문을 인준함

2013 년 6 월

위 원 장 \_\_\_\_\_ (인)

부위원장 \_\_\_\_\_ (인)

위 원 \_\_\_\_\_ (인)

## **Abstract**

# **Autofluorescence generation and elimination: a lesson from glutaraldehyde**

Kwahun Lee

Department of Science Education

(Major in Chemistry)

The Graduate School

Seoul National University

Autofluorescence, either emerging in biological imaging or nanomaterials synthesis is usually one of the unwanted fluorescence sources in spite of valuable usage as a featured signal in diagnostic tissue imaging of specific organelles. This

illudes the origin of target signal and significantly decrease the signal-to-noise ratio. The synthesis of luminescent nanomaterials also encounters the creation of unwanted emissive species in the presence of organic molecules. The unwanted emissive species might appear spectrally-pure but chemically-negligible when such organic molecules undergo extreme treatments such as oxidation, heating or microwaving, resulting in difficulty to assign the actual emissive species. Glutaraldehyde, widely used as fixative and cross-linking agents in bioimaging and biomedical engineering, causes especially high autofluorescence. We investigated the fluorogenic mechanism of glutaraldehyde. It reacted with proteins and synthetic peptides to generate visible to near-IR emitters. A model compound indicated that ethylenediamine and a secondary amine in the molecule are key components for the formation of emissive species. The proposed yellow emitter presented structural and photophysical similarity to the Cy3 dye. With current mechanism, the generation and elimination of autofluorescence can be controlled. Our results not only allow an explanation for the formation of unwanted emissive species during luminescent materials synthesis, but also a way to decrease autofluorescence in biological imaging.

**Key words:** glutaraldehyde, autofluorescence, ethylenediamine,

**Student number:** 2011-21581

# Contents

<b>I. Introduction .....</b>	<b>1</b>
<b>1.1. What is luminescence and why important? .....</b>	<b>1</b>
<b>1.2. Development of fluorophores .....</b>	<b>2</b>
<b>1.2.1. Criteria for a good fluorophore .....</b>	<b>2</b>
<b>1.2.2. Widely used fluorophores.....</b>	<b>4</b>
<b>1.2.2.1. Organic fluorophores.....</b>	<b>4</b>
<b>1.2.2.2. Inorganic fluorophores.....</b>	<b>6</b>
<b>1.3. Advancement of fluorescence microscopy and imaging techniques .....</b>	<b>9</b>
<b>1.3.1. Advantages of fluorescence imaging in chemical and biological studies .....</b>	<b>9</b>
<b>1.3.2. Advances in fluorescence imaging techniques.....</b>	<b>10</b>
<b>1.3.3. Strategies to minimize unwanted signals.....</b>	<b>13</b>

1.4. A model investigation of autofluorescence using glutaraldehyde .....	15
<b>II. Experimental Section .....</b>	<b>18</b>
<b>III. Results and Discussion .....</b>	<b>21</b>
<b>IV. Conclusion .....</b>	<b>39</b>
<b>V. References .....</b>	<b>40</b>
국문초록 .....	50

## List of Figures

<b>Figure 1.</b> Spectra of 1 mg/mL glutaraldehyde solutions in the presence of 1 mg/mL various organic species. ....	21
<b>Figure 2.</b> Fluorophore formation between glutaraldehyde and several organics. Histone at pH 7 (A) and pH 12 (B); <i>N</i> <sup>1</sup> -(3-(trimethoxysilyl)propyl)ethane-1,2-diamine (2) at pH 7 (C); diethylenetriamine (3) at pH 7 (D). ....	22
<b>Figure 3.</b> Spectral comparison of products between glutaraldehyde and various ethylenediamine derivatives. ....	25
<b>Figure 4.</b> Fluorophore formations between glutaraldehyde and diethylenetriamine (3) at pH 12 (A) and diethylenetriamine at pH 7 in phosphate buffer (B). ....	27
<b>Figure 5.</b> Influence of ionic concentration on the products of the reaction between glutaraldehyde and diethylenetriamine derivatives. "em <sub>xxx</sub> " indicates an emission spectrum at <i>xxx</i> nm excitation. Higher ion concentration generally promoted the formation of the red emitter. However, higher pH suppressed the generation of the red emitter. ....	28
<b>Figure 6.</b> Formation of the yellow between glutaraldehyde and <b>3</b> . (A). Absorption spectra at varied glutaraldehyde to <b>3</b> ratios. (B). The yellow emitter decayed but a blue emitter occurred. The intensity of the above two emitters was plotted versus time. ....	29

<b>Figure 7.</b> Mass spectrum of the HPLC purified mixture of glutaraldehyde and diethylenetriamine. ....	31
<b>Figure 8.</b> Formation of the yellow emitter between glutaraldehyde and <b>3</b> . (A) The yellow emitter decayed but a blue emitter occurred. (B) Spectra of the yellow emitter in regular and degassed solutions. ....	32
<b>Figure 9.</b> HPLC-Mass spectrum of the ion-exchange column-purified products of glutaraldehyde and diethylenetriamine. The top is the ion abundance spectrum; the middle is the mass at real time 2.72 min, matching the mass of 10 plus sodium; the bottom is the mass spectrum at real time <b>11.76</b> to 13.35, matching the mass of 11 (432.5 ) and a less dehydrated derivative of <b>11</b> (450.3) .....	34
<b>Figure 10.</b> Emission spectra of glutaraldehyde-fixed U2OS cells. The left panels are images merged from bright field and fluorescence images (upper left, pH 7; lower left, pH 12). Their fluorescence spectra are shown on the right...	35
<b>Figure 11.</b> Emission spectra of the yellow emitter in the presence of several reducing agents. (A) Borohydride (3 mM). The inset shows the solution colors before (pink) and after (yellow) reduction. (B) Glutathione (2 mM). (C) Hydroquinone (2 mM). (D) Ascorbic acid (6 mM).....	37

## List of schemes

<b>Scheme 1.</b> Structures of glutaraldehyde-reactive species.....	24
<b>Scheme 2.</b> Possible mechanism for the yellow emitter generation .....	30

## **I. Introduction**

### **1.1. What is luminescence and why important?**

Luminescence is defined as spontaneous emanation of radiation from excited species that is in a disequilibrium state with surroundings.<sup>1</sup> The excitation can emerge either from chemical reaction or radiation of light, i.e. absorption of photon. If the excitation of species was induced by absorption of photons, radiation from this excitation state is specifically called “photoluminescence”. Photoluminescence is one of the possible deactivation processes from the excited state. Radiative process (fluorescence, phosphorescence) and radiationless process (vibrational relaxation, internal conversion, external conversion, intersystem crossing) are examples of such processes.

Luminescence is useful as analytic signal in terms of sensitivity. The limit of detection from luminescence signal is 10 ~ 1000-fold better than that of absorption. In addition, large linear concentration range of luminescence is well associated with separation techniques to purify compounds.<sup>2,3</sup>

Fluorescence, as one of photoluminescences, can be utilized either in molecular probing or in cellular imaging about cell dynamics<sup>2</sup>. The excellent characters of luminescence incite researchers to improve luminescent detection technology, as well as to invent better fluorophores for higher quality of imaging.

## 1.2. Development of fluorophores

### 1.2.1. Criteria for a good fluorophore

Fluorophore is a molecular individual that emits fluorescence when it is excited by a proper wavelength of light.<sup>4</sup> Its major application is cellular staining and imaging. Many researchers have been trying to achieve flawless visualization of objects without distortion or fainting under unimpaired natural physiological condition<sup>5-8</sup>. This level of imaging techniques, of which ultimate goals are intact *in vivo* and single molecule imaging, cannot be accomplished without the development of excellent fluorophores.

To be an effective imaging agent, fluorophore possesses higher molar extinction coefficient ( $\epsilon$ ,  $M^{-1}\cdot cm^{-1}$ ), higher quantum yield ( $\Phi$ ), shorter fluorescence lifetime ( $\tau$ ), to yield higher brightness ( $B_e$ ) at given excitation and emission wavelength. Fluorophore with higher molar extinction coefficient absorbs photon more effectively even either when the concentration of fluorophore is low or when the intensity of radiated light is weak. Quantum yield is defined as a proportion of a certain deactivation way compared to the number of photons absorbed. In the case of fluorescence, it is described as follows.

$$\phi_F = \frac{k_{fluorescence}}{\sum k_i}$$

Where  $k_{fluorescence}$  is the rate of fluorescence, and  $\sum k_i$  is the sum of rates of possible deactivation ways.<sup>9</sup> High quantum yield of emission means the converged signals on emission rather than other signals such as heat. Shorter lifetime results in higher emission rate. Brightness, which is defined as multiplication of extinction coefficient and quantum yield ( $B_e = \varepsilon \times \phi$ ) at a particular wavelength, reflects the capacity of emitting light under a certain condition. In addition to those characters mentioned above, low photobleaching quantum yield, high chemical and photophysical stability<sup>10</sup>, and least possible transition to dark state<sup>11</sup>, where no fluorescence is observed, will enrich the quality of imaging much higher.

### **1.2.2. Widely used fluorophores.**

Popular fluorophores used in these days include organic dyes, fluorescent proteins, small size protein/peptides conjugated with organic dyes, metal-centered complexes, quantum dots, silver nanodots. They function as probes to detect not only non-fluorescent species, but also environmental factors such as pH, oxygen and metal ions.<sup>12</sup> Each type of fluorophore has its own advantages and disadvantages as an imaging agent. Concise properties of them are listed and discussed in the following sections.

#### **1.2.2.1. Organic fluorophores**

Small organic dyes are used for cellular staining. They are conjugated to antibodies to increase staining specificity. They are small, i.e. less than 1 nm, and some can permeate cells for direct cell staining. Fine adjustment of wavelength of excitation and emission can be achieved by simply changing side chains and type of organic dyes, such as rhodamine family<sup>13-16</sup>, alexa series<sup>17, 18</sup> and cyanine family<sup>19-22</sup>. Short lifetime (usually 1~10 ns), high quantum yield (3 ~ 100 %), reasonably good extinction coefficient ( $2.5 \times 10^4 \sim 2.5 \times 10^5 \text{ M}^{-1}\text{cm}^{-1}$ ), and good commercial availability are fetching characters of organic dyes that leads to wide applications.<sup>23</sup> On the other hand, several improvements still remain necessary. To be specific, poor

selectivity of organic dyes to proteins causes non-specific staining and increases background signals, and poor photostability under radiation still hampers long-term observation of objects.

Fluorescent proteins were developed to overcome non-specificity of organic dyes. Tagging of fluorescent proteins to protein of interest enables trafficking the location of proteins by observing its fluorescence.<sup>24, 25</sup> Not only their excellent specificity, but also high quantum yield (higher than 60 %), variety of available emission wavelength are also advantageous features.<sup>26, 27</sup> Representative paradigm of fluorescent protein is green fluorescent protein (GFP), of which variations include improvement of photostability, and progress to make it photoswitchable (on/off).<sup>28</sup> However, their relatively large size (> 3 nm) may cause steric hindrance to specific proteins, consequently to limit application diversity.

The problem due to fluorescent protein size was solved by conjugating organic dyes to small size protein/peptides, with assistance of enzyme in some cases.<sup>29, 30</sup> In this system, organic dyes play a role as labeling agent, and small size protein/peptides as genetically encoded tag to enhance specific staining. Thus, divergence of organic fluorophores and good specificity of genetic tags of small size protein/peptides make synergetic effect to visualize cellular environment. Examples that apply the systems are fusions between biarsenical dyes (FIAsH, ReAsH) and tetracysteine tag<sup>31</sup>, between Ni ion and hexahistidine tag<sup>32</sup>, and between O<sup>6</sup>-alkylguanine–DNA alkyltransferase and enzymatic substrate derivatives.<sup>33</sup> This

system, however, still lacks capability of employing substrate adapted with organic fluorophores for imaging cell in situ condition. In addition, photostability of fluorescent proteins are not sufficient for long-term imaging.

#### **1.2.2.2. Inorganic fluorophores**

One of efforts to utilize inorganic material for developing fluorophores is metal-centered complex. Transition metals with  $d^6$  or  $d^8$  electron configuration, such as Ru (II), Os (II), Re (I), Ir (III) and Pt (II), which emit light by metal-to-ligand-charge-transfer (MLCT),<sup>34-36</sup> are used in the system. Lanthanide (III) complexes also shows distinguished pointy emission arising from f-f electronic states transition.<sup>37, 38</sup> Relatively long lifetime ( $> \mu\text{s}$ ), large Stoke shift, narrow half maximum full width (HMF<sub>W</sub>,  $< 10 \text{ nm}$ ), relatively high quantum yield.<sup>39</sup> However, these complexes lack selectivity when used for chemical sensing. In addition their dependence of emission on oxygen makes their application only conditional. In other words, cell staining of metal-centered complex needs high dose of chromophores, but staining is still irregular.<sup>40-42</sup>

Semiconductor quantum dots (QDs) have been considered as a promising fluorophore due to their excellent photophysical properties. Together with tunable emission wavelength (400 nm – 1000 nm and above) with changing particle size and composition of particles<sup>43</sup>, excellent photostability, high molar extinction coefficient

( $10^5$ – $10^6$   $M^{-1} \text{ cm}^{-1}$ ), high quantum yield (10-100 % (visible), 20-70 % (NIR)), reasonably long lifetime (10~100 ns) lead to variety of applications that cover single molecule imaging, cellular imaging, and even *in vivo* imaging.<sup>23, 43-49</sup> On the contrary, blinking of semiconductor quantum dots is critical impediment for steady single molecular imaging. Moreover, subordination of their properties on surface modification enlarges their hydrodynamic diameter up to 60 nm, which is not suitable for cell-permeation process. A number of biomolecules conjugated on the surface of quantum dot may sterically impede target molecules and eventually induce aggregation. These barriers make delivery of quantum dot to target molecules harder. Thus, they either have to be carried in physical way such as microinjection<sup>50</sup> or in chemical way by further conjugation to cell penetrating peptide.<sup>51</sup> In addition, possibility of releasing toxic heavy metal from nanoparticle such as free cadmium still urges supplementary actions, because degradation of CdS quantum dots are reported under illumination,<sup>52</sup> oxidation,<sup>53, 54</sup> or by hypochlorous acid.<sup>55</sup> The latter is abundant biological oxidant in inflammatory tissues.

Silver nanodots, a new type of fluorophore that is comprised of few-atom clusters of reduced silver,<sup>56</sup> are comparable to semiconductor quantum dots to the respect of photophysical properties. Possible emission wavelength of silver nanodots encompasses blue (440 nm) to near IR (900 nm). Their high quantum yield (up to 40 %), good extinction coefficient ( $1.2 \times 10^5 \sim 9.5 \times 10^5$   $M^{-1} \text{ cm}^{-1}$ ), excellent photostability (more than 60-fold stable than organic dyes) together with short

lifetime (0.01 ~ 4.3 ns), and excellent two photon absorption cross section (50,000 GM, Goppert-Mayer units,  $10^{-50} \text{ cm}^4 \text{ photon s}^{-1}$ ) while retaining small size (~ 2 nm) gather increasing attention to the particle. Elucidation of structures and improvement of photophysical properties are on rapid progress and the scope of biological application, such as probes and bio-labeling, are gradually expanding.<sup>57-63</sup> Even though staining of fixed cell with silver nanodots has been demonstrated<sup>61</sup>, live cell imaging is still challenging due to luminescence quenching by compounds, such as chloride and other biocomponents<sup>64, 65</sup>, under physiological condition. Also, chemical yield of fluorescent silver nanodots is so low, which means high proportion of non-fluorescent silver-protecting group (single strand DNA, polymer, peptides) complexes are formed in the synthesis and they will compete when they are used to stain cells.

### **1.3. Advancement of fluorescence microscopy and imaging techniques**

#### **1.3.1. Advantages of fluorescence imaging in chemical and biological studies**

Fluorescence imaging with microscopy is one of promising techniques with high sensitivity and specificity. The scope of fluorescence imaging ranges from envisioning surface of tissues at molecular level to visualize complete organism without distortion, even though scattering of incident light is still problematic to achieve such resolution. This method is particularly useful because molecular level of imaging can be acquired in a relatively noninvasive way and synergetic effect can be made when used with other highly-sensitive imaging techniques, such as x-ray, MRI (Magnetic Resonance Imaging), and CT (Computed tomography).<sup>48</sup> It is a versatile device that not only enables vivid imaging of living cells and tissues as main purpose, but also enables investigation of chemical systems. To be specific, polymer blends, liquid crystals, colloid could be the object of fluorescence imaging.<sup>66</sup> Along with developing better fluorophore, advancement of fluorescence imaging techniques also proceeds both at microscopic, which bestows resolution surpassing the diffraction limit (typically 0.2~ 0.3  $\mu\text{m}$ ), and at macroscopic level, which allows molecular imaging of small-body-animals.<sup>8</sup> Moreover, many methods to increase signal to noise ratio also have been investigated.

### 1.3.2. Advances in fluorescence imaging techniques<sup>66</sup>

In conventional fluorescence microscope, a specific wavelength of excitation light is selected by interference filter or by a monochromator after radiated by mercury or xenon lamp. Radiated specimen with a proper light gives emission that is detected usually with either eyes or CCD (Charge-coupled device) camera. Penetration depth of ordinary fluorescence microscope is 2~ 3  $\mu\text{m}$  and highest resolution is limited to 0.2~0.3  $\mu\text{m}$  which corresponds to half wavelength of the light source. Moreover, the noise is a large factor that causes low signal-to-noise ratio. Overcoming these limitations calls for emerging of equipments with higher signal-to-noise ratio such as confocal microscopy, two-photon excitation microscopy as well as near-field scanning optical microscopy (NSOM) for higher resolution.

Restriction of resolution of conventional microscope, roughly half wavelength of incident light, is subdued by locating specimen near the newly introduced sub-wavelength light source in Near-field scanning optical microscope (NSOM). A hole with diameter shorter than wavelength of light interacts with the surface of adjacent sample before the light experiences diffusion. This simple principle, called “near-field optics”, was proven to be sufficiently powerful to achieve single molecules and have been expanding its field. High resolution, capacity for mapping of surface and abated photobleaching are advantageous character of NSOM. As a simple system,

NSOM is not only capable of observing thin films such as electroluminescent polymers, liquid crystals and Langmuir-Blodgett films, but also systems encompassing photosynthetic systems, chromosome mapping, protein localization.

Confocal microscope adopts a pinhole as a way to select more of relevant signal and to discard irrelevant signals. A pinhole in a confocal microscope only allows properly focused fluorescence, among emission emerged from specimen, to pass through and contributes to signal. This pinhole system makes it possible to obtain three dimensional images with 0.5  $\mu\text{m}$  z-axial resolution. Light radiated from lasers is detected by vibrating mirrors or rotating disks that have many pinholes. Lasers are used as light source and that induces faster photobleaching of specimen under observation. Diminishing laser power, utilizing more stable fluorophore, enhancing sensitivity of detector, higher objective numerical aperture is possible means to increase signal intensity and likely reduce photobleaching. Popular fields of application of confocal microscopy in cell biology are imaging of single cells varies from envision of organelles to electrical potential distribution,  $\text{Ca}^{2+}$  imaging and so on.

Two-photon excitation fluorescence microscopy<sup>67</sup> is distinguished from normal fluorescence spectroscopy in that two photons with lower energy are absorbed contemporarily to excite a fluorophore. Normally, a fluorophore is excited only when a photon with same energy as energy gap between ground state and excited state is absorbed. Excitation from two photons, of which time interval is less than

$10^{-18}$  s, offers fascinating features of two-photon system. Since cross section of two-photon absorption is confined to an area where flux of photon is large enough to excite adjacent fluorophore, possibility of two-photon absorption is low. In addition, reliance of Two-photon excitation on excitation light intensity is quadratic, which means that excitation intensity decreases by the square of the distance from the focal plane. If z-axis is considered, probability decreases by fourth power of distance. These low possibilities of excitation and high sensitivity to incident light intensity constrain excitation volume to supply inherent three dimensional resolution. To be specific, roughly 80 % of light excited at 780 nm with numerical aperture of objective 1.25 can be converged in 1  $\mu\text{m}$  of the focal plane, and excitation volume of two-photon absorption is about a ten billionth to that of normal fluorescence microscopy. This restrained excitation region, together with low incident light energy, guarantee to achieve higher signal-to-noise ratio under investigation. Furthermore, if excitation light is located in Near-IR position, deeper penetration depth and higher signal-to-noise ratio can be acquired, because of Near IR optical windows where less absorption from tissues are expected.<sup>5</sup> Moreover, small excitation volume is helpful to avoid unnecessary mitigation of incident radiation intensity by out-of-focusing, so precise control of incipient light also is possible.

### **1.3.3. Strategies to minimize unwanted signals**

Other than improving microscopic resolution, efforts to minimizing irrelevant signals to gain higher signal-to-noise ratio also have been exerted. As one of signals that hamper precise fluorescence imaging of cell, autofluorescence has been a target that is to be avoided with various strategies.

“Autofluorescence” is the term that describes the fluorescence originated from cells or tissues discerned from the fluorescence signal from exogenous compounds. It is widely known that molecules such as reduced Nicotinamide adenine dinucleotide (NAD(P)H), lipopigments, flavins and proteins that comprise of amino acids containing with aromatic groups shows intrinsic fluorescence signal.<sup>68</sup> In addition, fixatives that contain aldehyde groups, such as glutaraldehyde and malondialdehyde, also induce fluorescence signal. Even though this unexpected fluorescence is not bothersome in regular cell imaging, it becomes problematic when the fluorescence signal from target molecule is dim. That is the reason that many methods have been proposed to avoid autofluorescence.

First of all, exploitation of time-gated microscopy can reduce background signal by collecting emission signals at different timing from when autofluorescence prevails.<sup>59</sup> The signal is collected either before or after autofluorescence become prevalent. In the similar way, fluorophores with discriminating lifetime can be selected to minimize overlap between expected signals and background.<sup>69, 70</sup>

Developing fluorophores with Near-IR emission is in line with this strategy<sup>71</sup>, because absorption from autofluorescence in that region is weaker than other regions. Additionally, reduction with borohydride is a popular way people have been used to diminish autofluorescence.<sup>72</sup> Using quenching agents such as Evan blue<sup>73</sup>, schiff's reagents reduced with sodium borohydride<sup>74</sup>, pontamine sky blue<sup>75</sup> also efficient to decrease the background signals. Lastly, optical modulation of microscopy with secondary laser excitation also was helpful to decline the effect of autofluorescence.<sup>76</sup>

In line with the aforementioned approaches, reactions between glutaraldehyde and small organic compounds as model compounds were chosen to simulate generation and elimination of autofluorescence in fixed cells. This approach is distinguishable in that, instead of merely presenting a way to control autofluorescence, it proposes the mechanism of the generation of autofluorescence, together with a way to eliminate autofluorescence.<sup>77</sup> The proposed mechanism bestows a fundamental perspective on the autofluorescence as well as controlling the generation of autofluorescence.

#### **1.4. A model investigation of autofluorescence using glutaraldehyde.**

The importance of fluorescence for many chemical and biological studies cannot be stressed enough<sup>12, 48, 78, 79</sup>. However, autofluorescence that often appears in nanomaterial synthesis and biological imaging<sup>68, 80-82</sup> has made researchers be suffered. First of all, this phenomenon emerges when organic molecules are used in the synthesizing emissive nanomaterials, and become even more apparent when they are under extreme treatments such as heating or microwaving. Even though their amounts are negligible in chemically, this unwanted emissive species might affect the spectrum of the intended product, which make it difficult to ascribe the particles that give emission. Scrutinizing the mechanism of fluorogenic reactions may help us to explain the unexpected generation of fluorophores during nanomaterial synthesis. Similar phenomenon occurred in cellular matrix also could be analyzed.

In spite of its valuable usage as a featured signal in diagnostic tissue imaging of specific organelles<sup>83-86</sup>, autofluorescence considered as an obstacle because it considerably declines signal-to-noise ratio to interfere other fluorescence signal reading<sup>87, 88</sup>. Many methods have been applied to reduce the hindrance. It is usually increased after fixation with glutaraldehyde<sup>73</sup> and other biological materials<sup>89, 90</sup>.

Glutaraldehyde is a dialdehyde that is vastly used as a cross-linking agent. Widespread usage of glutaraldehyde is originated not only from its highest reactivity among mono- or dialdehyde groups<sup>91</sup>, but also from its commercial availability and

low cost. Thus, it is natural that utilization of glutaraldehyde in fixation of live cell<sup>92</sup> and its reaction with nucleic acids<sup>93</sup>, tissue lipids<sup>94</sup>, protein<sup>95</sup> have vastly been studied. Studies have shown the ability of glutaraldehyde as materials for bioimaging and biomedical engineering including protein cross-linking reagent<sup>96</sup>, enzyme and protein immobilization<sup>95,97,98</sup>, sterilization<sup>99</sup>, drug delivery<sup>100</sup>. However, significantly higher autofluorescence is induced when glutaraldehyde is used to fix cell.<sup>101</sup> Higher reactivity of dialdehyde may contribute to this phenomenon. Furthermore, glutaraldehyde is easily polymerized at neutral or alkaline pH due to aldol condensation reaction,<sup>102</sup> resulting in multicomponent mixtures of oligomers, including  $\alpha$ ,  $\beta$ -unsaturated aldehydes as well as cyclic hemiacetal of its hydrates.<sup>103-107</sup> That is the reason why the main reactive species in the aqueous solution still remains controversial although there's been extensive investigation on the mechanism that glutaraldehyde works, and only handful of literatures are available concerning the reaction of glutaraldehyde especially above pH 10.<sup>108-110</sup> Whereas fixation of cells and tissues is still indispensable in histology and cell biology, the structural retaining ability of glutaraldehyde for small molecules such as antigens<sup>111</sup>, amino acids, and small peptides<sup>112</sup> enables continuous manipulation.<sup>74</sup> It is not clear yet how such a higher autofluorescence background occurs.

Herein, a new fluorophore based on the reaction between polyglutaraldehyde and primary amino groups, which are connected covalently in a single step, was synthesized in alkaline aqueous solution. This investigation will lead us to better

understanding the mechanism for the autofluorescence originated from glutaraldehyde. Photophysical and chemical properties was analyzed and the structure of new compound was estimated.

## II. Experimental Section

### 2.1. Reagents

Glutaraldehyde (grade I, 70% in H<sub>2</sub>O, specially purified for use as an electron microscopy fixative or other sophisticated use) and diethylenetriamine (ReagentPlus®, 99%) and Triethylenetetramine hydrate (98 %), ethylenediamine (ReagentPlus®, 99%), N-(3-Trimethoxysilylpropyl) diethylenetriamine, N-[3-(Trimethoxysilyl)propyl]ethylenediamine (97 %), histone from calf thymus (Type II-A, lyophilized powder), L-Ascorbic acid (bioextra, CRYSTALLINE), CM Cellulose, Phosphate buffered saline, L-glutathionine reduced (>98 %) and hydroquinone were purchased from Sigma-Aldrich and used in as received. Ammonia (28~30 % aqueous solution) was purchased from Samchun chemicals in Korea.

## 2.2. Synthesis of fluorophores

All samples were prepared either in PBS or deionized water (18M $\Omega$ ). The effect of ionic strength on the synthesis of fluorophore was conducted by comparing samples made out of solutions with different ion concentration. In general, glutaraldehyde and other compounds with amine groups, such as diethylenetriamine, triethylenetetramine, Trimethoxysilyl propyl zdiethylenetriamine , N-[3-(Trimethoxysilyl)propyl]ethylenediamine (97%) and histone were mixed in the aqueous solution (molar ratio glutaraldehyde: compounds with amino group = 2:1) at pH 12 and stayed in the dark at room temperature for 24 hours.

In terms of purification, samples were concentrated through lyophilizing (Ilshin Lab, TFD 5505) and then purified with Ion exchange column (CM Cellulose). 90 mM ~ 100 mM NH<sub>3</sub> solution was used as eluent. Samples were further analyzed with HPLC-MS system (acetonitrile/water, MSI-MS system (LCQ)).

Reducing agents, such as sodium borohydride, L-Ascorbic acid, L-glutathionine reduced, hydroquinone, were added to the sample at a molar ratio of glutaraldehyde and reducing agents at 1:1.

Measuring quantum yield was conducted by comparing to Rhodamine 6G. Emission spectra and absorption spectra were obtained with QM-40 (Photon Technology International, Inc.) and S-4100 (SCINCO), respectively.

Freeze-and-thaw method was used to degas. Nitrogen gas was refilled after degassing steps to prevent inflow of oxygen from the air, and sample was left at room temperature before taking spectra.

Live cell was fixed by 2 wt % glutaraldehyde dissolved in PBS solution (pH 7, pH 13) and their autofluorescence was measured by confocal microscope (Carl Zeiss LSM710) under 514 nm laser excitation.

### III. Results and discussion

Cellular protein and synthetic peptides are glutaraldehyde reactive. Commercially available glutaraldehyde exhibits weak blue emission, likely due to impurities (Fig. 1A.). The reaction between glutaraldehyde and histone, a common protein in cells, yielded a green emitter in neutral solution ( $\lambda_{\text{ex}}/\lambda_{\text{em}} = 475 \text{ nm}/525 \text{ nm}$ ) (Fig. 2A). At higher pH, however, a yellow emitter was formed ( $\lambda_{\text{ex}}/\lambda_{\text{em}} = 535 \text{ nm}/555 \text{ nm}$ ) (Fig. 2B). Since histone is rich in lysine and arginine, poly-L-lysine (**polyK**) and poly-L-arginine (**polyR**) were examined. Interestingly, **polyR** (MW 4000–15 000) and glutaraldehyde produced a yellow emitter ( $\lambda_{\text{ex}}/\lambda_{\text{em}} = 515 \text{ nm}/585 \text{ nm}$ ) and a blue emitter ( $\lambda_{\text{ex}}/\lambda_{\text{em}} = 370 \text{ nm}/411 \text{ nm}$ ) (Fig. 1F). Small peptide **polyK** (MW 1000–4000) only induced weak blue emission. However, larger **polyK** (MW 4000–15 000) led to the formation of a weak red emitter ( $\lambda_{\text{ex}}/\lambda_{\text{em}} = 575 \text{ nm}/625 \text{ nm}$ ) and a strong yellow emitter ( $\lambda_{\text{ex}}/\lambda_{\text{em}} = 534 \text{ nm}/555 \text{ nm}$ ) that was observed in the products of glutaraldehyde and histone mixture (Fig. 1C and D). The generation of similar emitters in both **polyK** and histone may suggest that a lysine residue, or an amino group is the key component for yellow fluorophore formation. Synthetic peptides with more hydrophobic residues, such as **LSHK** (LSHKTCTLKLTCTKHSL), only generated weak blue emission. However, peptides such as **KECD** (KECDKKECDKKECDK) yielded higher yellow and green emitters, in which the green emitter was the same as that of histone (Fig. 1B and E).

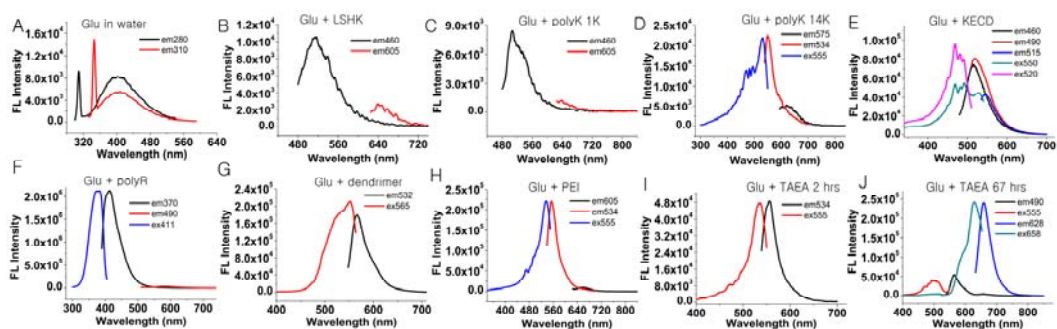


**Figure 1.** Spectra of 1 mg/mL glutaraldehyde solutions in the presence of 1 mg/mL various organic species. “Glu” represents glutaraldehyde. "em xxx" indicates an emission spectrum at xxx nm excitation. Similarly, "ex xxx" stands for an excitation spectrum at xxx nm detection. A. Aqueous glutaraldehyde solution (max 400 nm). The emission is likely due to impurities. B. With peptide LSHK (LSHKTCTLKLTCTKHSL), showing weak green (max 515 nm) and red emission (max 645 nm). C. With peptide poly-L-lysine (MW 1 K to 4 K), showing weak green emission (max 515 nm). D. With peptide poly-L-lysine (MW 4 K to 15 K), showing weak yellow (max 550 nm) and red emission (max 625 nm). E. With peptide KECD (KECDKKECDKKECDK), showing medium green (max 518 nm) and weak yellow emission (max 545 nm). F. With peptide poly-L-arginine (MW 4 K to 15 K), showing strong blue emission (max 412 nm). G. With PAMAM dendrimer, ethylenediamine core, generation 2.0, showing medium yellow emission (max 567 nm). H. With PEI (Poly(ethyleneimine)) (MW 2 K), showing medium yellow emission(max 555 nm). I. With Tris(2-aminoethyl)amine, showing weak yellow emission(max 555nm) in two hours. K. With Tris(2-aminoethyl)amine, showing weak yellow (max 565 nm) and mediumred emission (max 656 nm) in 67 hours.

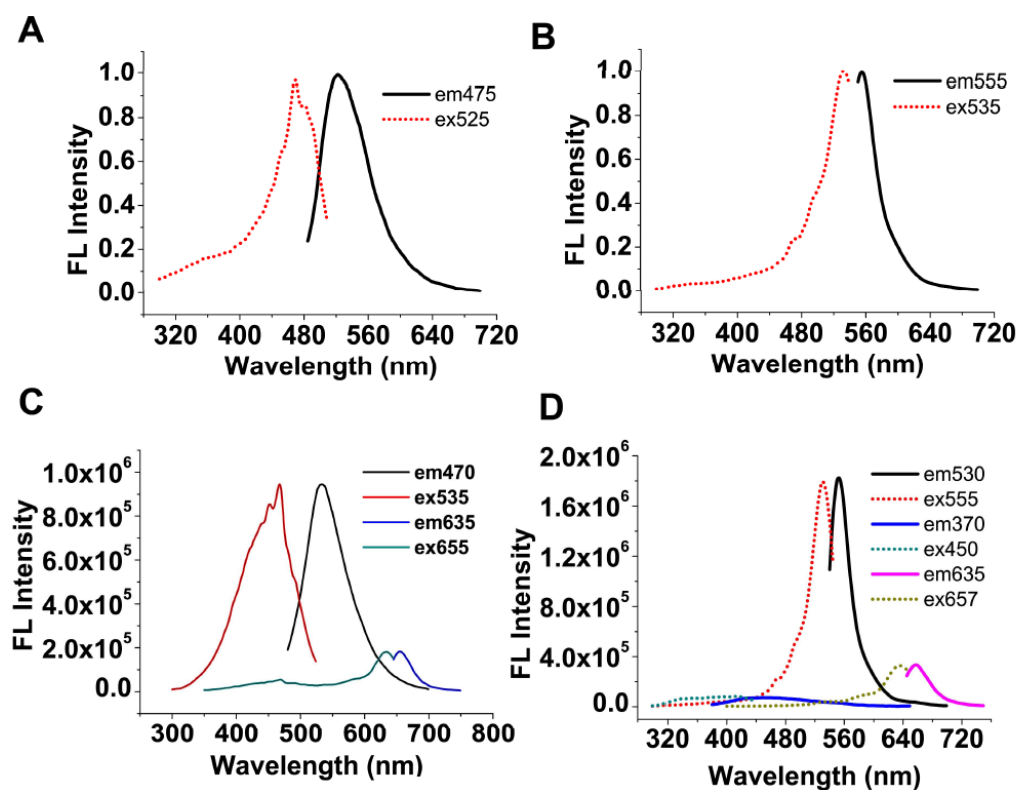
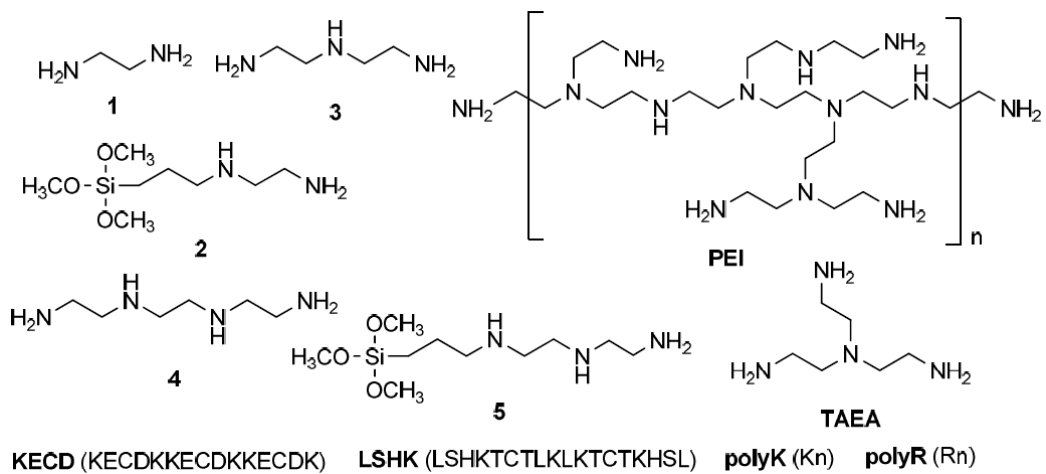


**Figure 2.** Fluorophore formation between glutaraldehyde and several organics. Histone at pH 7 (A) and pH 12 (B); *N'*-(3-(trimethoxysilyl)propyl)ethane-1,2-diamine (**2**) at pH 7 (C); diethylenetriamine (**3**) at pH 7 (D). “emxxx” indicates an emission spectrum at xxx nm excitation. Similarly, “exxxx” stands for an excitation spectrum at xxx nm detection.

The example of **KECD** suggested that the participation of amino and carboxylic acid groups also facilitated the fluorophore formation.

Given that the amino group appeared in the above peptides, we utilized small amino molecules to investigate the function of amino groups (Scheme 1). Both simple ammonia and ethane-1,2-diamine (**1**) did not lead to the formation of emissive species. However, when one of the amino groups was replaced by secondary amine, such as *N*<sup>1</sup>-(3-(trimethoxysilyl)-propyl)ethane-1,2-diamine (**2**), a green emitter ( $\lambda_{\text{ex}}/\lambda_{\text{em}} = 470 \text{ nm}/535 \text{ nm}$ ) similar to that of histone in neutral solution was generated (Fig. 2C). It appears that the presence of secondary amine was critical for the fluorophore formation. With an extra amino group in the molecule, diethylenetriamine (**3**) formed a red emitter ( $\lambda_{\text{ex}}/\lambda_{\text{em}} = 635 \text{ nm}/657 \text{ nm}$ ) and a yellow emitter ( $\lambda_{\text{ex}}/\lambda_{\text{em}} = 530 \text{ nm}/555 \text{ nm}$ ) in the presence of glutaraldehyde. The latter emitter exhibited the same spectrum as that of the above histone derivative (Fig. 2D). Other molecules with repeated ethylenediamine characteristics, such as *N*<sup>1</sup>,*N*<sup>1'</sup>-(ethane-1,2-diyl)-diethane-1,2-diamine (**4**), *N*<sup>1</sup>-(2-aminoethyl)-*N*<sup>2</sup>-(3-(trimethoxysilyl)-propyl)ethane-1,2-diamine (**5**), *N*<sup>1</sup>, *N*<sup>1'</sup>-bis(2-aminoethyl)ethane-1,2-diamine (**TAEA**) and poly(ethyleneimine) (**PEI**) also reacted with glutaraldehyde to form emissive species (Fig. 1H–J and 3).



**Scheme 1.** Structures of glutaraldehyde-reactive species

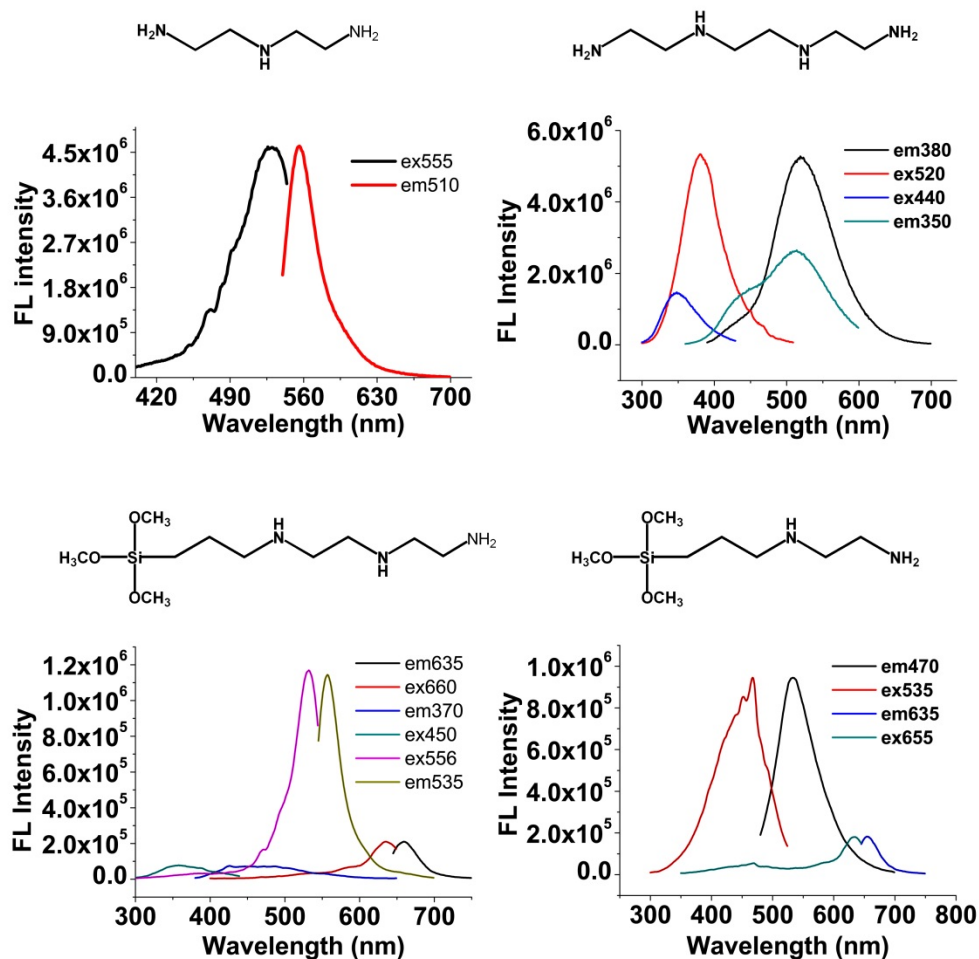


**Figure 3.** Spectral comparison of products between glutaraldehyde and various ethylenediamine derivatives. "emxxx" indicates an emission spectrum at xxx nm excitation. Similarly, "exxxx" stands for an excitation spectrum at xxx nm detection. Structurally similar amine derivatives, such as **2** and **4** as well as **3** and **5**, yielded similar spectra.

Such fluorogenic reactions can be controlled by several factors. Higher ionic strength promoted the generation of red emitters (Fig. 4B and 5). However, higher pH suppressed the generation of red emitter, and accelerated the formation of the yellow emitter, resulting in relatively spectrally pure solution (Fig. 4A). We therefore used diethylenetriamine **3** as a model compound to investigate the mechanism of the yellow emitter formation. A ratio of 3: 1 for glutaraldehyde to ethylenediamine yielded better emission intensity. Excess glutaraldehyde induced the generation of non-emissive species, as indicated by the strong absorption in the UV region (Fig. 6A). Since two glutaraldehyde molecules tend to form  $\alpha$ ,  $\beta$ -unsaturated aldehyde in basic solution,<sup>105, 106</sup> the aldol condensation reaction product **6** may react with amine **3** to produce  $\alpha$ ,  $\beta$ -unsaturated Schiff base **7** (Scheme 2),<sup>113</sup> which was easily detected using mass spectrometry (Fig. 7). The basic environment may induce addition of the hydroxyl ion to imine to yield **8**.<sup>114</sup> The fact that a secondary amine is a prerequisite for the formation of the yellow emitter corroborates the transition to **9**. Following dehydration reaction of the hydroxyl group, the formation of the yellow emitter requires oxidation of **9** to yield **10**, resulting in a donor–acceptor-flanked polymethine structure. The final step was supported by the experiment that removal of oxygen suppressed the formation of the yellow emitter (Fig. 8B). It might not be a rate-determining step but **9** was rather

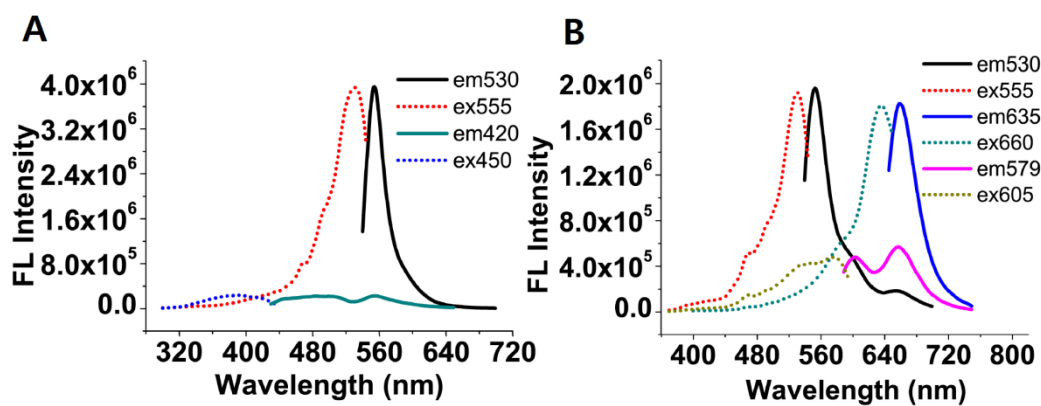


**Figure 4.** Fluorophore formations between glutaraldehyde and diethylenetriamine (**3**) at pH 12 (A) and diethylenetriamine at pH 7 in phosphate buffer (B). "emxxx" indicates an emission spectrum at xxx nm excitation. Similarly, "exxxx" stands for an excitation spectrum at xxx nm detection.

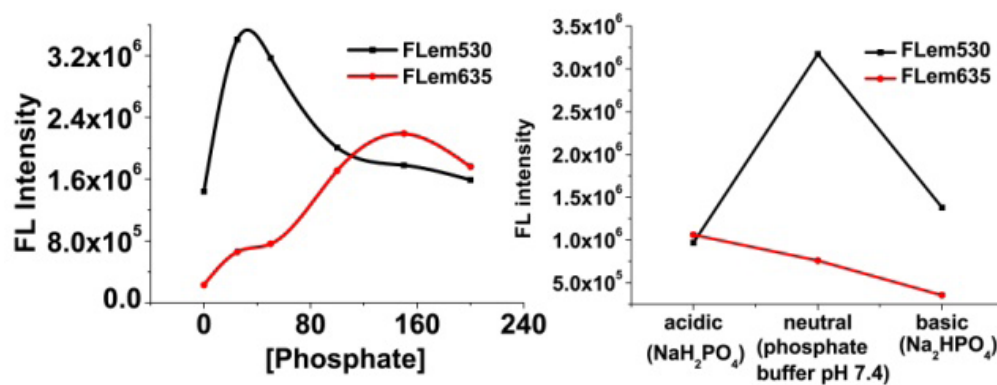


**Figure 5.** Influence of ionic concentration on the products of the reaction between glutaraldehyde and diethylenetriamine derivatives. "emxxx" indicates an emission spectrum at xxx nm excitation. Higher ion concentration generally promoted the formation of the red emitter. However, higher pH suppressed the generation of the red emitter.

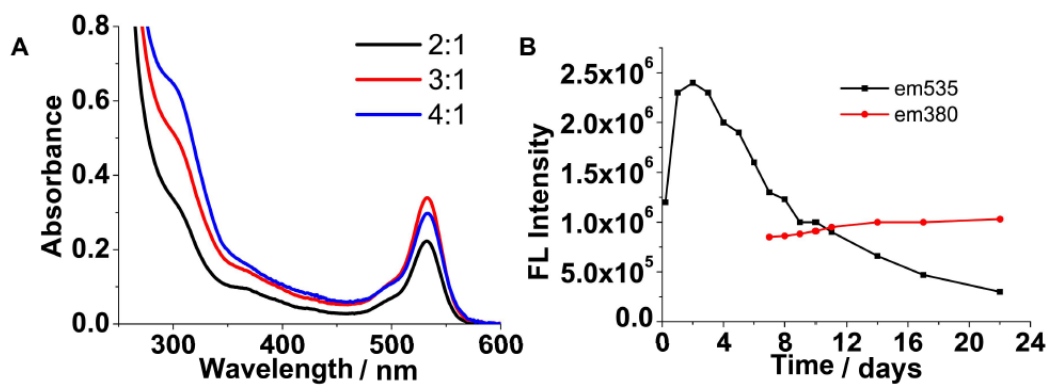
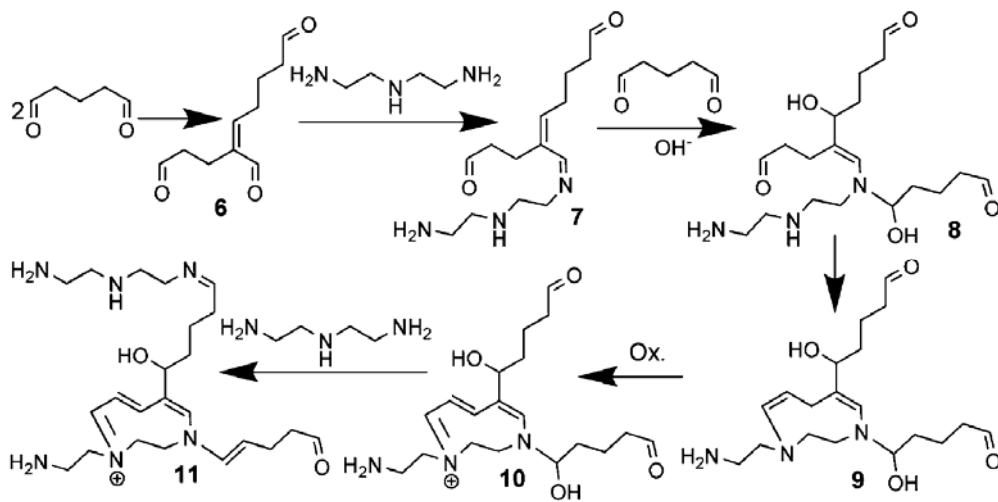


**Figure 6.** Formation of the yellow between glutaraldehyde and **3**. (A) Absorption spectra at varied glutaraldehyde to **3** ratios. (B) The yellow emitter decayed but a blue emitter occurred. The intensity of the above two emitters was plotted versus time.



**Scheme 2.** Possible mechanism for the yellow emitter generation

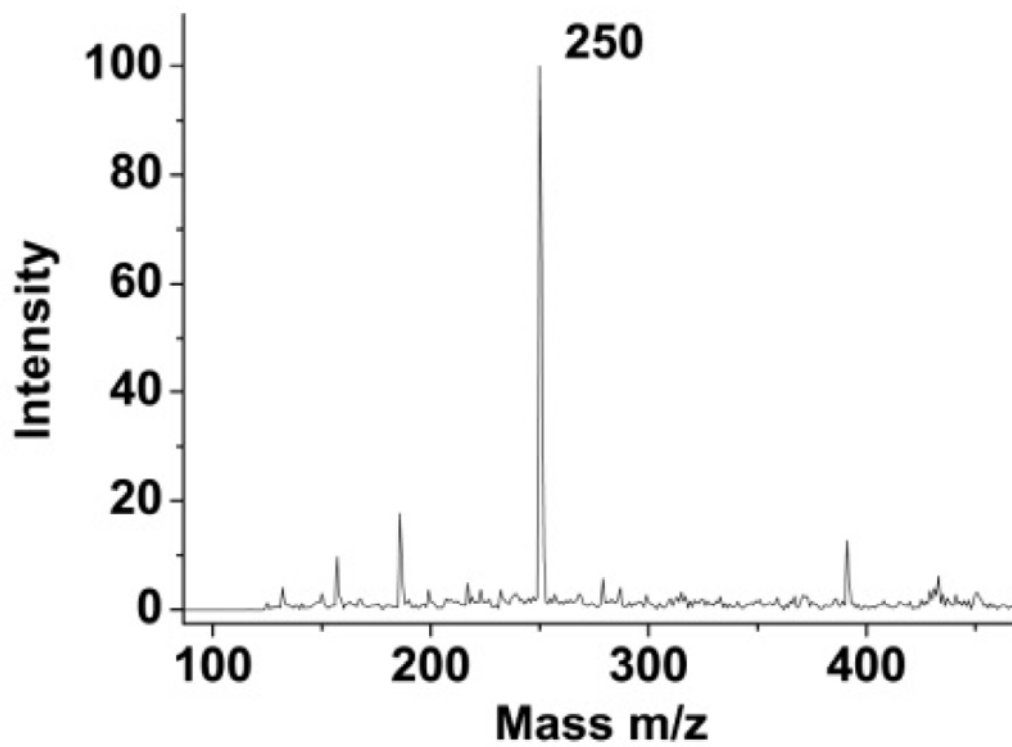


**Figure 7.** Mass spectrum of the HPLC purified mixture of glutaraldehyde and diethylenetriamine.

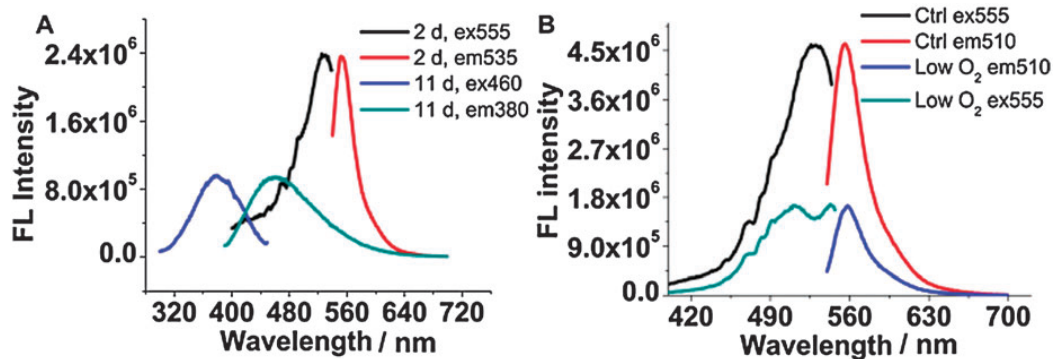


**Figure 8.** Formation of the yellow emitter between glutaraldehyde and **3**. (A) The yellow emitter decayed but a blue emitter occurred. (B) Spectra of the yellow emitter in regular and degassed solutions.

easily oxidisable since small amounts of leaking oxygen still facilitated the yellow emitter formation.

Interestingly, the proposed structure for the yellow emitter exhibited similar structural and photophysical properties to those of the Cy3 dye, for example, 7% quantum yield and short lifetime (0.2 ns). Given the similar extinction coefficient to Cy3, the chemical yield of such a fluorophore was less than 0.5%. The yellow emitter showed only moderate stability, and decayed gradually to a blue emitter ( $\lambda_{\text{ex}}/\lambda_{\text{em}} = 380 \text{ nm}/460 \text{ nm}$ ) (Fig. 8A). The low chemical yield and co-existence of many derivatives due to the reactive amino and aldehyde groups in the molecule, just like autofluorescence in cells, imposed further difficulty in purification. However, the detection of **10** (ESMS+:  $m/z$  388.8 (M + Na)) and its derivatives such as **11** (ESMS+:  $m/z$  432.5 (M+)) with HPLC-MS confirmed the existence of the above key structure (Fig. 9).

Many methods have been applied to reduce the interference from autofluorescence by either chemical or physical methods.<sup>59, 115</sup> The current model helped us to understand the fluorogenic mechanism of glutaraldehyde and in return to avoid strong autofluorescence of glutaraldehyde-fixed biomaterials. For example, higher pH will promote the generation of the yellow emitter, resulting in higher autofluorescence under blue or green excitation from glutaraldehyde-fixed cells at pH 12, double that of pH 7. A neutral fixative, however, yielded multi-emissions, though with lower intensity (Fig. 10).

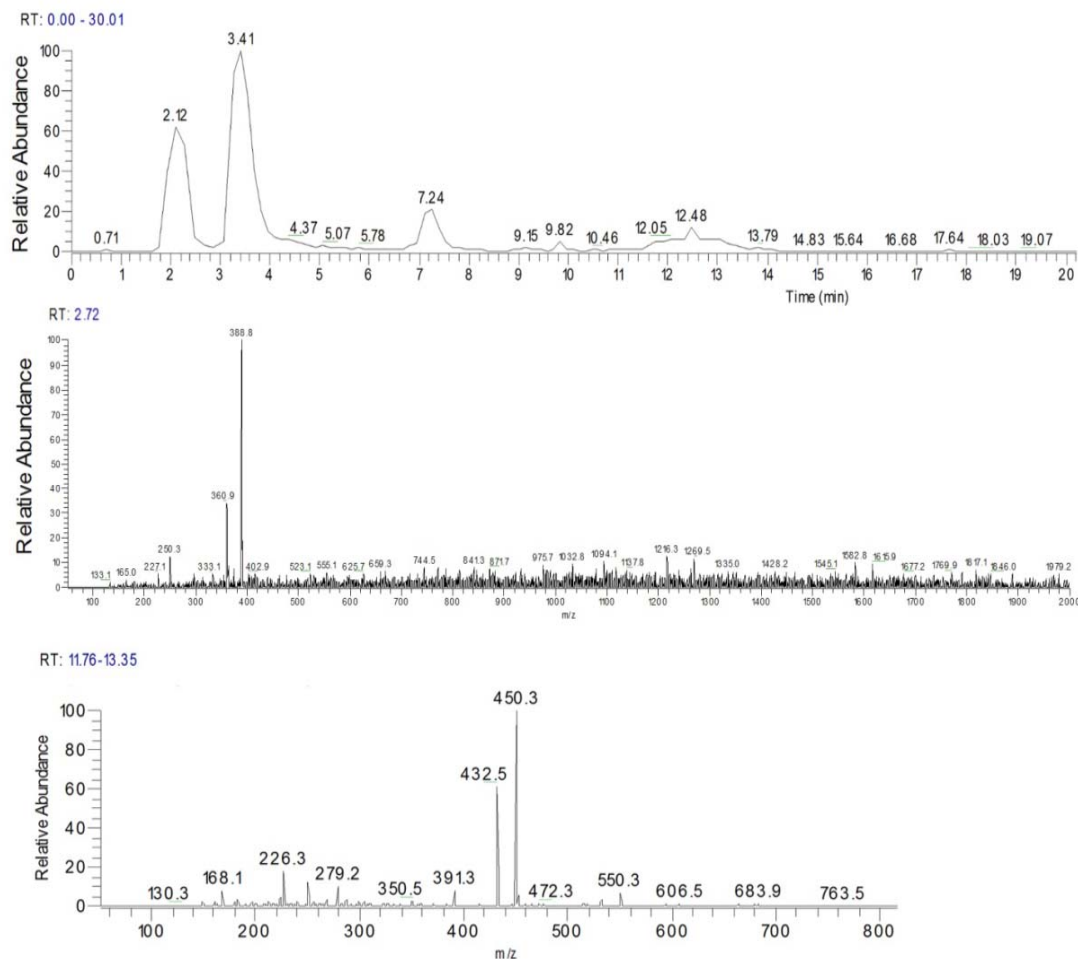


**Figure 9.** HPLC-Mass spectrum of the ion-exchange column-purified products of glutaraldehyde and diethylenetriamine. The top is the ion abundance spectrum; the middle is the mass at real time 2.72 min, matching the mass of **10** plus sodium; the bottom is the mass spectrum at real time **11.76** to **13.35**, matching the mass of **11** (432.5) and a less dehydrated derivative of **11** (450.3).

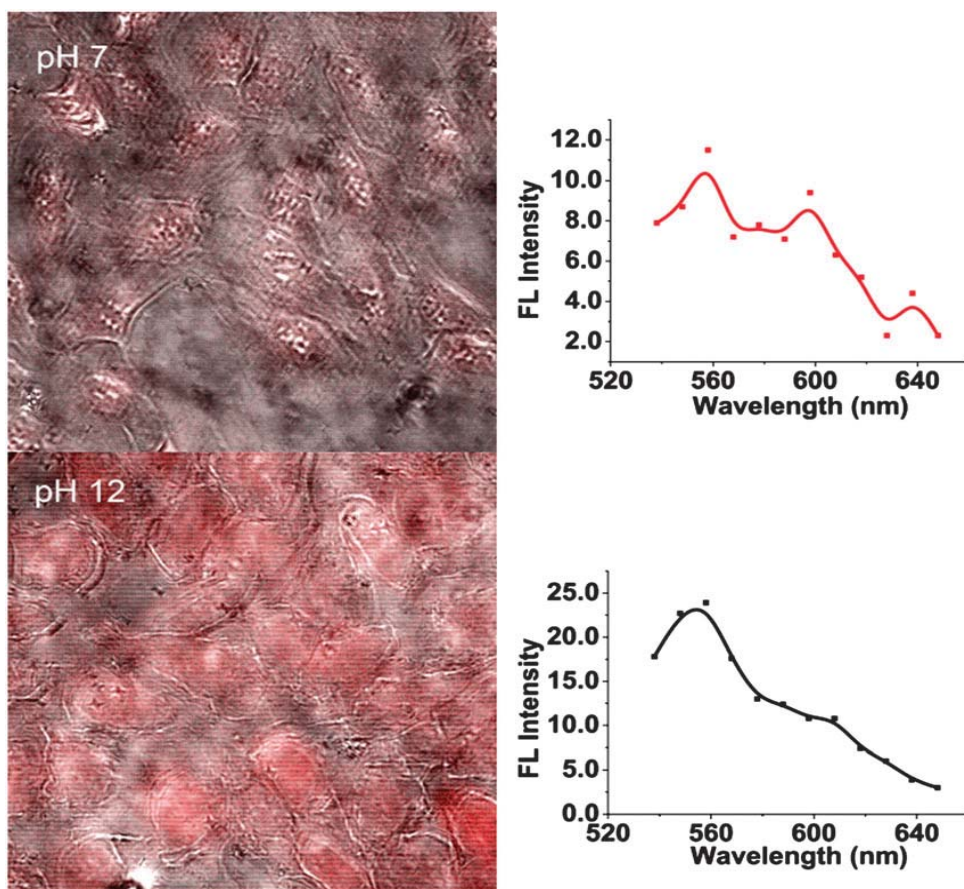


**Figure 10.** Emission spectra of glutaraldehyde-fixed U2OS cells. The left panels are images merged from bright field and fluorescence images (upper left, pH 7; lower left, pH 12). Their fluorescence spectra are shown on the right.

Based on our model, some tissue imaging techniques also received theoretical evidence. Sodium borohydride has been widely used on fixed cells/tissues to eliminate autofluorescence.<sup>116</sup> Its reduction capability was considered to play a role. When sodium borohydride was added to a solution of the yellow emitter, the pink solution became yellow while the yellow emission decreased. However, it seems that borohydride is not a perfect agent, since the blue peak at 460 nm increased slightly (Fig. 11A). Glutathione only decreased the yellow emission instantly to a lower intensity following its addition (Fig. 11B). In contrast, ascorbic acid increased both the blue and the yellow emission (Fig. 11D). Surprisingly, hydroquinone eliminated all the fluorescence (Fig. 11C). As far as we know, this is the first report that hydroquinone can decrease autofluorescence interference. The elimination of the fluorescence is likely due to the reduction of the fluorophores by hydroquinone. At higher pH, all the fluorescence disappeared after incubation with hydroquinone. However, lowering the pH to 7 induced extra fluorescence peaks. Our discovery was in line with the fact that the reduction potential of hydroquinone strongly depends on pH.<sup>117, 118</sup>

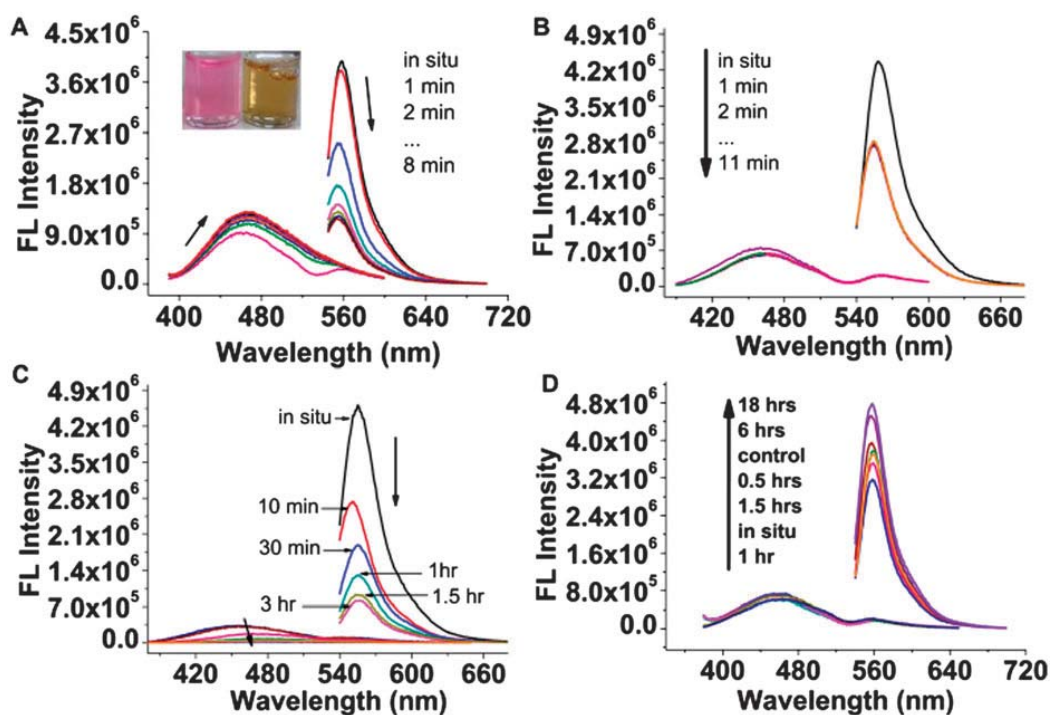


**Figure 11.** Emission spectra of the yellow emitter in the presence of several reducing agents. (A) Borohydride (3 mM). The inset shows the solution colors before (pink) and after (yellow) reduction. (B) Glutathione (2 mM). (C) Hydroquinone (2 mM). (D) Ascorbic acid (6 mM).

## **IV. Conclusion**

The fluorogenic mechanism of autofluorescence induced by glutaraldehyde was investigated. Ethylenediamine and a secondary amine in the molecule are key components in the formation of emissive species with glutaraldehyde. The proposed yellow emitter that was produced from the reactions between glutaraldehyde and histone, synthetic peptides or ethylenediamine derivatives, presented structural and photophysical similarity to Cy3 dye. The generation and elimination of autofluorescence were also discussed. Our results not only provide methods to decrease autofluorescence in biological imaging, but also help us to explain the unwanted emissive species during luminescent materials synthesis.

## V. References

1. PAC, 68, 2223 *Glossary of terms used in photochemistry (IUPAC Recommendations 1996)*.
2. B. Douglas A. Skoog; F. James Holler; Stanley R. Crouch, *Principles of instrumental analysis* 6th edn., 2006.
3. J. H. M. Sauer, and J. Enderlein, *Handbook of Fluorescence Spectroscopy and Imaging*, WILEY-VCH Verlag GmbH & Co. , KGaA, Weinheim, 2011.
4. PAC, 79, 293 *Glossary of terms used in photochemistry, 3rd edition (IUPAC Recommendations 2006)*.
5. J. V. Frangioni, *Curr Opin Chem Biol*, 2003, **7**, 626-634.
6. J. Rao, A. Dragulescu-Andrasi and H. Yao, *Curr Opin Biotechnol*, 2007, **18**, 17-25.
7. P. P. Ghoroghchian, M. J. Therien and D. A. Hammer, *Wiley Interdiscip Rev Nanomed Nanobiotechnol*, 2009, **1**, 156-167.
8. V. Ntziachristos, *Annu Rev Biomed Eng*, 2006, **8**, 1-33.
9. N. J. Turro, V. Ramamurthy and J. C. Scaiano, *Photochem Photobiol*, 2012, **88**, 1033-1033.
10. S. Weiss, *Science*, 1999, **283**, 1676-1683.
11. S. A. Patel, M. Cozzuol, J. M. Hales, C. I. Richards, M. Sartin, J. C. Hsiang, T. Vosch, J. W. Perry and R. M. Dickson, *J Phys Chem C Nanomater Interfaces*, 2009, **113**, 20264-20270.

12. M. Schaferling, *Angew Chem Int Ed Engl*, 2012, **51**, 3532-3554.
13. M. Orrit and J. Bernard, *Phys Rev Lett*, 1990, **65**, 2716-2719.
14. E. Betzig and R. J. Chichester, *Science*, 1993, **262**, 1422-1425.
15. P. R. Selvin, T. Ha, T. Enderle, D. F. Ogletree, D. S. Chemla and S. Weiss, *Biophys J*, 1996, **70**, Wp302-Wp302.
16. X. H. Xu and E. S. Yeung, *Science*, 1997, **275**, 1106-1109.
17. R. Dave, D. S. Terry, J. B. Munro and S. C. Blanchard, *Biophys J*, 2009, **96**, 2371-2381.
18. C. C. Fu, H. Y. Lee, K. Chen, T. S. Lim, H. Y. Wu, P. K. Lin, P. K. Wei, P. H. Tsao, H. C. Chang and W. Fann, *Proc Natl Acad Sci U S A*, 2007, **104**, 727-732.
19. T. Funatsu, Y. Harada, M. Tokunaga, K. Saito and T. Yanagida, *Nature*, 1995, **374**, 555-559.
20. X. Zhuang, L. E. Bartley, H. P. Babcock, R. Russell, T. Ha, D. Herschlag and S. Chu, *Science*, 2000, **288**, 2048-2051.
21. M. Ueda, Y. Sako, T. Tanaka, P. Devreotes and T. Yanagida, *Science*, 2001, **294**, 864-867.
22. Y. Sako, S. Minoghchi and T. Yanagida, *Nat Cell Biol*, 2000, **2**, 168-172.
23. U. Resch-Genger, M. Grabolle, S. Cavaliere-Jaricot, R. Nitschke and T. Nann, *Nat Methods*, 2008, **5**, 763-775.
24. D. M. Chudakov, S. Lukyanov and K. A. Lukyanov, *Trends Biotechnol*, 2005, **23**, 605-613.
25. J. Livet, T. A. Weissman, H. Kang, R. W. Draft, J. Lu, R. A. Bennis, J. R. Sanes

- and J. W. Lichtman, *Nature*, 2007, **450**, 56-62.
26. M. F. Garcia-Parajo, G. M. Segers-Nolten, J. A. Veerman, J. Greve and N. F. van Hulst, *Proc Natl Acad Sci U S A*, 2000, **97**, 7237-7242.
  27. A. A. Heikal, S. T. Hess, G. S. Baird, R. Y. Tsien and W. W. Webb, *Proc Natl Acad Sci U S A*, 2000, **97**, 14831-14831.
  28. K. A. Lukyanov, D. M. Chudakov, S. Lukyanov and V. V. Verkhusha, *Nat Rev Mol Cell Biol*, 2005, **6**, 885-891.
  29. H. M. O'Hare, K. Johnsson and A. Gautier, *Curr Opin Struct Biol*, 2007, **17**, 488-494.
  30. N. Johnsson and K. Johnsson, *Acs Chemical Biology*, 2007, **2**, 31-38.
  31. B. A. Griffin, S. R. Adams and R. Y. Tsien, *Science*, 1998, **281**, 269-272.
  32. E. G. Guignet, R. Hovius and H. Vogel, *Nat Biotechnol*, 2004, **22**, 440-444.
  33. A. Keppler, S. Gendreizig, T. Gronemeyer, H. Pick, H. Vogel and K. Johnsson, *Nat Biotechnol*, 2003, **21**, 86-89.
  34. K. K. Lo, T. K. Lee, J. S. Lau, W. L. Poon and S. H. Cheng, *Inorg Chem*, 2008, **47**, 200-208.
  35. K. K. W. Lo, K. H. K. Tsang, K. S. Sze, C. K. Chung, T. K. M. Lee, K. Y. Zhang, W. K. Hui, C. K. Li, J. S. Y. Lau, D. C. M. Ng and N. Zhu, *Coordin Chem Rev*, 2007, **251**, 2292-2310.
  36. E. Rajalakshmanan and V. Alexander, *Inorg Chem*, 2007, **46**, 6252-6260.
  37. D. Parker, R. S. Dickins, H. Puschmann, C. Crossland and J. A. K. Howard, *Chem Rev*, 2002, **102**, 1977-2010.

38. C. P. Montgomery, B. S. Murray, E. J. New, R. Pal and D. Parker, *Acc Chem Res*, 2009, **42**, 925-937.
39. J. Yu, D. Parker, R. Pal, R. A. Poole and M. J. Cann, *J Am Chem Soc*, 2006, **128**, 2294-2299.
40. E. J. New, D. Parker, D. G. Smith and J. W. Walton, *Curr Opin Chem Biol*, 2010, **14**, 238-246.
41. J. L. Vinkenborg, M. S. Koay and M. Merckx, *Curr Opin Chem Biol*, 2010, **14**, 231-237.
42. M. R. Gill, J. Garcia-Lara, S. J. Foster, C. Smythe, G. Battaglia and J. A. Thomas, *Nature Chem*, 2009, **1**, 662-667.
43. X. Michalet, F. F. Pinaud, L. A. Bentolila, J. M. Tsay, S. Doose, J. J. Li, G. Sundaresan, A. M. Wu, S. S. Gambhir and S. Weiss, *Science*, 2005, **307**, 538-544.
44. I. L. Medintz, H. T. Uyeda, E. R. Goldman and H. Mattoussi, *Nat Mater*, 2005, **4**, 435-446.
45. X. Gao, L. Yang, J. A. Petros, F. F. Marshall, J. W. Simons and S. Nie, *Curr Opin Biotechnol*, 2005, **16**, 63-72.
46. S. Nie, Y. Xing, G. J. Kim and J. W. Simons, *Annu Rev Biomed Eng*, 2007, **9**, 257-288.
47. A. P. Alivisatos, *Science*, 1996, **271**, 933-937.
48. B. N. Giepmans, S. R. Adams, M. H. Ellisman and R. Y. Tsien, *Science*, 2006, **312**, 217-224.

49. D. R. Larson, W. R. Zipfel, R. M. Williams, S. W. Clark, M. P. Bruchez, F. W. Wise and W. W. Webb, *Science*, 2003, **300**, 1434-1436.
50. J. B. Delehanty, H. Mattoussi and I. L. Medintz, *Anal Bioanal Chem*, 2009, **393**, 1091-1105.
51. I. L. Medintz, T. Pons, J. B. Delehanty, K. Susumu, F. M. Brunel, P. E. Dawson and H. Mattoussi, *Bioconjug Chem*, 2008, **19**, 1785-1795.
52. Y. Zhang, J. He, P. N. Wang, J. Y. Chen, Z. J. Lu, D. R. Lu, J. Guo, C. C. Wang and W. L. Yang, *J Am Chem Soc*, 2006, **128**, 13396-13401.
53. A. Hoshino, K. Fujioka, T. Oku, M. Suga, Y. F. Sasaki, T. Ohta, M. Yasuhara, K. Suzuki and K. Yamamoto, *Nano Lett.*, 2004, **4**, 2163-2169.
54. J. Ma, J.-Y. Chen, J. Guo, C. C. Wang, W. L. Yang, L. Xu and P. N. Wang, *Nanotechnology*, 2006, **17**, 2083-2089.
55. M. C. Mancini, B. A. Kairdolf, A. M. Smith and S. Nie, *J Am Chem Soc*, 2008, **130**, 10836-10837.
56. S. Choi, R. M. Dickson and J. Yu, *Chem Soc Rev*, 2012, **41**, 1867-1891.
57. Y. Antoku, J. Hotta, H. Mizuno, R. M. Dickson, J. Hofkens and T. Vosch, *Photochem Photobiol Sci*, 2010, **9**, 716-721.
58. S. Choi, J. Yu, S. A. Patel, Y. L. Tzeng and R. M. Dickson, *Photochem Photobiol Sci*, 2011, **10**, 109-115.
59. J. Yu, S. A. Patel and R. M. Dickson, *Angew Chem Int Ed Engl*, 2007, **46**, 2028-2030.
60. J. H. Yu, S. Choi and R. M. Dickson, *Angew Chem Int Ed Engl*, 2009, **48**, 318-

320.

61. J. Yu, S. Choi, C. I. Richards, Y. Antoku and R. M. Dickson, *Photochem Photobiol*, 2008, **84**, 1435-1439.
62. W. Guo, J. Yuan, Q. Dong and E. Wang, *J Am Chem Soc*, 2010, **132**, 932-934.
63. J. S. Hsin-Chih Yeh , Jason J. Han , Jennifer S. Martinez \* and James H. Werner, *Nano Lett.*, 2010, **10**, 3106-3110.
64. P. Roussel and D. Hernandez-Verdun, *Exp Cell Res*, 1994, **214**, 465-472.
65. K. F. S. Luk, A. H. Maki and R. J. Hoover, *J Am Chem Soc*, 1975, **97**, 1241-1242.
66. B. Valeur, *Molecular Fluorescence: Principles and Applications*, Wiley-VCH Verlag GmbH, 2002.
67. P. T. So, C. Y. Dong, B. R. Masters and K. M. Berland, *Annu Rev Biomed Eng*, 2000, **2**, 399-429.
68. M. Monici, in *Biotechnol Annu Rev*, ed. M. R. El-Gewely, Elsevier, 2005, vol. 11, pp. 227-256.
69. L. O. Palsson, R. Pal, B. S. Murray, D. Parker and A. Beeby, *Dalton Trans*, 2007, 5726-5734.
70. J. Wu, G. Wang, D. Jin, J. Yuan, Y. Guan and J. Piper, *Chem Commun (Camb)*, 2008, 365-367.
71. M. Mörtelmaier, E. J. Kögler, J. Hesse, M. Sonnleitner, L. A. Huber and G. J. Schütz, *Single molecules*, 2002, **3**, 225-231.
72. B. Clancy and L. J. Cauler, *J Neurosci Methods*, 1998, **83**, 97-102.

73. J. A. Werkmeister, T. A. Tebb, D. E. Peters and J. A. M. Ramshaw, *Clin Mater*, 1990, **6**, 13-20.
74. P. Tagliaferro, C. J. Tandler, A. J. Ramos, J. Pecci Saavedra and A. Brusco, *J Neurosci Methods*, 1997, **77**, 191-197.
75. T. Cowen, A. J. Haven and G. Burnstock, *Histochemistry*, 1985, **82**, 205-208.
76. C. I. Richards, J. C. Hsiang, D. Senapati, S. Patel, J. Yu, T. Vosch and R. M. Dickson, *J Am Chem Soc*, 2009, **131**, 4619-4621.
77. K. Lee, S. Choi, C. Yang, H. C. Wu and J. Yu, *Chem Commun (Camb)*, 2013, **49**, 3028-3030.
78. A. Miyawaki, *Annu Rev Biochem*, 2011, **80**, 357-373.
79. A. Okamoto, *Chem Soc Rev*, 2011, **40**, 5815-5828.
80. R. B. Restani, P. I. Morgado, M. P. Ribeiro, I. J. Correia, A. Aguiar-Ricardo and V. D. Bonifacio, *Angew Chem Int Ed Engl*, 2012, **51**, 5162-5165.
81. D. Wang and T. Imae, *J Am Chem Soc*, 2004, **126**, 13204-13205.
82. I. Georgakoudi, B. C. Jacobson, M. G. Muller, E. E. Sheets, K. Badizadegan, D. L. Carr-Locke, C. P. Crum, C. W. Boone, R. R. Dasari, J. Van Dam and M. S. Feld, *Cancer Research*, 2002, **62**, 682-687.
83. B. B. Theyel, D. A. Llano, N. P. Issa, A. K. Mallik and S. M. Sherman, *Nat Protoc*, 2011, **6**, 502-508.
84. J. M. Levitt, M. Hunter, C. Mujat, M. McLaughlin-Drubin, K. Munger and I. Georgakoudi, *Opt Lett*, 2007, **32**, 3305-3307.
85. W. T. Chang, Y. C. Yang, H. H. Lu, I. L. Li and I. Liao, *J Am Chem Soc*, 2010,

- 132**, 1744-1745.
86. X. Shao, W. Zheng and Z. Huang, *Opt Express*, 2010, **18**, 24293-24300.
  87. Y. Fu, J. Zhang and J. R. Lakowicz, *Photochem Photobiol*, 2009, **85**, 646-651.
  88. M. Mörtelmaier, E. J. Kögler, J. Hesse, M. Sonnleitner, L. A. Huber and a. G. J. Schütz, *Single molecules*, 2002, **3**, 225-231.
  89. K. A. Zukor, D. T. Kent and S. J. Odelberg, *Dev Dyn*, 2010, **239**, 3048-3057.
  90. J. H. Dowson, *Histochemie*, 1973, **37**, 75-79.
  91. J. H. Bowes and C. W. Cater, *Biochim Biophys Acta*, 1968, **168**, 341-352.
  92. D. HOPWOOD, *Histochem J*, 1972, **4**, 267-303.
  93. D. Hopwood, *Histochem J*, 1975, **7**, 267-276.
  94. R. Gigg and S. Payne, *Chem Phys Lipids*, 1969, **3**, 292-295.
  95. A. J. Habeeb and R. Hiramoto, *Arch Biochem Biophys*, 1968, **126**, 16-26.
  96. F. M. RICHARDS and J. R. KNOWLES, *J. Mol. Biol.* , 1968, **37**, 231-233.
  97. E. F. Jansen, Y. Tomimatsu and A. C. Olson, *Arch Biochem Biophys*, 1971, **144**, 394-400.
  98. F. A. Quioco and F. M. Richards, *Biochemistry*, 1966, **5**, 4062-4076.
  99. S. P. Gorman, E. M. Scott and A. D. Russell, *J Appl Bacteriol*, 1980, **48**, 161-190.
  100. A. Jayakrishnan and S. R. Jameela, *Biomaterials*, 1996, **17**, 471-484.
  101. R. Bacallao, S. Sohrab and C. Phillips, *Guiding Principles of Specimen Preservation for Confocal Fluorescence Microscopy*, Springer, New York, 2006.
  102. K. Okuda, I. Urabe, Y. Yamada and H. Okada, *Journal of Fermentation and*

- Bioengineering*, 1991, **71**, 100-105.
103. F. M. Richards and J. R. Knowles, *J Mol Biol*, 1968, **37**, 231-&.
104. J. Kawahara, T. Ohmori, T. Ohkubo, S. Hattori and M. Kawamura, *Anal Biochem*, 1992, **201**, 94-98.
105. P. M. Hardy, A. C. Nicholls and H. N. Rydon, *J Chem Soc Chem Comm*, 1969, 565.
106. T. Tashima, M. Imai, Y. Kuroda, S. Yagi and T. Nakagawa, *J Org Chem*, 1991, **56**, 694-697.
107. S. Margel and A. Rembaum, *Macromolecules*, 1980, **13**, 19-24.
108. A. Rembaum, S. Margel and J. Levy, *J Immunol Methods*, 1978, **24**, 239-250.
109. A. D. Mcleod, F. C. Lam, P. K. Gupta and C. T. Hung, *J Pharm Sci*, 1988, **77**, 704-710.
110. S. Margel, *J Polym Sci Pol Chem*, 2003, **22**, 3521-3533.
111. J. T. Boyer, *Nature*, 1967, **214**, 291-292.
112. P. Tagliaferro, C. J. Tandler, A. J. Ramos, J. P. Saavedra and A. Brusco, *Journal of Neuroscience Methods*, 1997, **77**, 191-197.
113. I. Migneault, C. Dartiguenave, M. J. Bertrand and K. C. Waldron, *Biotechniques*, 2004, **37**, 790-796, 798-802.
114. P. M. Hardy, G. J. Hughes and H. N. Rydon, *J Chem Soc Perk T 1*, 1979, 2282-2288.
115. J. R. Mansfield and C. S. Maki, *Laboratory Investigation*, 2010, **90**, 342a-342a.
116. W. Baschong, R. Suetterlin and R. H. Laeng, *J Histochem Cytochem*, 2001, **49**,

1565-1572.

117. Carmichael and S. T. K. Mander, *J Histochem Cytochem*, 1967, **15**, 404-408.
118. S. I. Bailey, I. M. Ritchie and F. R. Hewgill, *J Chem Soc Perk T 2*, 1983, 645-652.

## 국문초록

자가형광은 생물을 영상화하거나 나노재료를 합성할 때 생겨난다. 이 신호는 때로 특정 세포소기관의 조직을 관찰하는데 사용되기도 하지만 대개의 경우 달갑지 않은 형광 신호 중 하나이다. 자가형광은 생물을 관찰할 때 형광 신호가 나오는 근원지를 모호하게 만들 뿐만 아니라, 현저하게 원하는 신호에 대한 불필요한 신호의 세기 (signal-to-noise)를 증가시킨다. 이에 더하여 유기 물질을 이용하여 형광을 발산하는 나노재료를 합성할 때 역시 이러한 원치 않는 신호가 나오게 된다. 이러한 원치 않는 형광을 방출하는 물질은 화학적으로는 무시해도 될 정도의 양이고 스펙트럼 상에서는 다른 것과 겹치지 않는다. 하지만 유기물을 산화시키거나 마이크로파, 또는 열을 가하여 극한의 조건으로 다루게 되면 생기는 원치 않는 형광은 실제로 형광을 발산하는 물질을 규정하고 관찰하는 것을 어렵게 만든다. 글루타알데히드는 생물을 영상화할 때나 생의학적인 공학기술에 접착제 혹은 가교결합 중개물질로 널리 쓰이는 물질인데, 다른 물질들에 비해 특별히 높은 정도의 자가 형광을 발현하는 것으로 알려져 있다. 이 연구에서는 글루타알데히드가 형광을 만드는 기작을 연구하였다. 글루타알데히드는 단백질이나 인조 펩타이드와 반응하여 가시광선과 근적외선 영역의 방사체를 만들었다. 모델로 삼은 화합물의 반응은

반응물의 에틸렌디아민(ethylenediamine)과 2 차 아민이 형광물질을 만드는 주요 요소임을 드러냈다. 이를 기반으로 제안된 노란색 형광을 내는 물질은 Cy3 dye 와 아주 비슷한 분자구조와 광물리적 성질을 나타냈다. 여기서 드러난 반응물의 기작을 자가 형광의 발생과 제거를 제어할 수 있는 방법을 제시하는데 이용하였다. 이 결과는 형광 재료물질을 생산하는데 생기는 원치 않는 형광 신호에 대한 정보를 제시해줄 뿐만 아니라, 생물을 영상화 하면서 자가 형광을 줄일 수 있는 방법 또한 제공한다.

**주요어** : 글루타알데히드, 자가 형광, 에틸렌디아민

**학번** : 2011-21581